

Enhanced cellular migration and prolonged chondrogenic differentiation in decellularized cartilage scaffolds under dynamic culture conditions


Eva Goldberg Bockhorn, Ulla Wenzel, Marie Nicole Theodoraki, Johannes Döscher, Ricarda Riepl, Marlene C. Wigand, Cornelia Brunner, Martin Heßling, Thomas K. Hoffmann, Johann Kern, Nicole Rotter

Angaben zur Veröffentlichung / Publication details:

Goldberg Bockhorn, Eva, Ulla Wenzel, Marie Nicole Theodoraki, Johannes Döscher, Ricarda Riepl, Marlene C. Wigand, Cornelia Brunner, et al. 2022. "Enhanced cellular migration and prolonged chondrogenic differentiation in decellularized cartilage scaffolds under dynamic culture conditions." *Journal of Tissue Engineering and Regenerative Medicine* 16 (1): 36–50. <https://doi.org/10.1002/term.3261>.

RESEARCH ARTICLE

Enhanced cellular migration and prolonged chondrogenic differentiation in decellularized cartilage scaffolds under dynamic culture conditions

Eva Goldberg-Bockhorn¹  | Ulla Wenzel² | Marie-Nicole Theodoraki¹ | Johannes Döscher¹ | Ricarda Riepl¹ | Marlene C. Wigand¹ | Cornelia Brunner¹ | Martin Heßling² | Thomas K. Hoffmann¹ | Johann Kern³ | Nicole Rotter³

¹Department of Otorhinolaryngology, Head and Neck Surgery, Ulm University Medical Center, Ulm, Germany

²Institute of Medical Engineering and Mechatronics, Ulm University of Applied Sciences, Ulm, Germany

³Department of Otorhinolaryngology, Head and Neck Surgery, Mannheim University Medical Center Heidelberg University, Mannheim, Germany

Correspondence

Eva Goldberg-Bockhorn, Department of Otorhinolaryngology, Head and Neck Surgery, Ulm University Medical Center, Frauensteige 12, 89075 Ulm, Germany.
Email: eva.goldberg@uniklinik-ulm.de

Funding information

Bundesministerium für Bildung und Forschung
Open access funding enabled and organized by Projekt DEAL

Summary

Lesions of aural, nasal and tracheal cartilage are frequently reconstructed by complex surgeries which are based on harvesting autologous cartilage from other locations such as the rib. Cartilage tissue engineering (CTE) is regarded as a promising alternative to attain vital cartilage. Nevertheless, CTE with nearly natural properties poses a significant challenge to research due to the complex reciprocal interactions between cells and extracellular matrix which have to be imitated and which are still not fully understood. Thus, we used a custom-made glass bioreactor to enhance cell migration into decellularized porcine cartilage scaffolds (DECM) and mimic physiological conditions. The DECM seeded with human nasal chondrocytes (HPCH) were cultured in the glass reactor for 6 weeks and examined by histological and immunohistochemical staining, biochemical analyses and real time-PCR at 14, 28 and 42 days. The migration depth and the number of migrated cells were quantified by computational analysis. Compared to the static cultivation, the dynamic culture (DC) fostered migration of HPCH into deeper tissue layers. Furthermore, cultivation in the bioreactor enhanced differentiation of the cells during the first 14 days, but differentiation diminished in the course of further cultivation. We consider the DC in the presented bioreactor as a promising tool to facilitate CTE and to help to better understand the complex physiological processes during cartilage regeneration. Maintaining differentiation of chondrocytes and improving cellular migration by further optimizing culture conditions is an important prerequisite for future clinical application.

KEYWORDS

bioreactors, cartilage, cell differentiation, chondrocytes, dynamic 3D cultivation, extracellular matrix, tissue engineering, xenogeneic implant matrix

Dr. Eva Goldberg-Bockhorn and Ulla Wenzel contributed equally to this manuscript and should be considered joint first author.

This is an open access article under the terms of the Creative Commons Attribution-NonCommercial License, which permits use, distribution and reproduction in any medium, provided the original work is properly cited and is not used for commercial purposes.

© 2021 The Authors. Journal of Tissue Engineering and Regenerative Medicine published by John Wiley & Sons Ltd.

1 | INTRODUCTION

Cartilage is a relatively simple tissue consisting of chondrocytes and a characteristic extracellular matrix (ECM). The latter plays an important role in mediating structural and functional processes within the tissue which are specific for each cartilage type (Benders et al., 2013; Bos et al., 2018; Swinehart & Badylak, 2016). While articular cartilage has to absorb shocks and reduce friction between the articular surfaces, the major role of cartilage in the head and neck region is to stabilize the shape of the pinna, nose and trachea to keep up the function of the particular organ. Congenital or acquired cartilaginous defects of the ear and nose have often to be repaired by complex operations in which cartilage transplants from other locations of the body have to be applied. The common side effects of these current standard methods are donor site morbidity such as pain, scars and deformity after cartilage harvesting (Mischkowski et al., 2008; Varadharajan et al., 2015) and a high expenditure of time. Alloplastic materials, which are less frequently used as an alternative material, are available unlimitedly but carry the risk of infection, rejection reactions or extrusion (Berghaus, 2007; Kim et al., 2014; Liang et al., 2018). Therefore, new strategies have to be developed to find an optimal solution for cartilage replacement. Tissue engineering, which is a field of worldwide experimental and partly clinically applied research, seems to be the most promising option. A large quantity of ECM based materials has been developed to restore lost cartilage (Benders et al., 2013). The advantages of those decellularized cartilage matrices are the availability of a stable framework for migrating cells as well as the biodegradability of the material on the one hand and the capability to induce cell signaling pathways by chemokines and cytokines to facilitate cell migration and differentiation on the other hand (Swinehart & Badylak, 2016). The ECM of porcine nasal septal cartilage as well as human nasal septal cartilage mainly consist of collagen type II (COL2A1) (Eyre & Muir, 1975; Popko et al., 2007). As known from comparative studies with auricular cartilage, the amount of glycosaminoglycans (GAG) may vary between human and porcine cartilage while the size of the lacunae and the mechanical properties of the cartilage seem to be comparable (Chiu et al., 2017). Therefore, decellularized porcine cartilage matrix (DECM) is supposed to be an optimal scaffold for Cartilage tissue engineering (CTE) due to its similar structure and properties. Porcine cartilage provides an almost limitless source of ECM for CTE and, as it has no cytotoxic effects, for the future application in vivo to restore absent cartilage in the head and neck region (Elsaesser et al., 2014; Schwarz et al., 2012, 2015). Preceding research showed an auspicious migration of chondrocytes into the porous but biomechanically stable DECM as well as a positive matrix synthesis and matrix interaction (Goldberg-Bockhorn et al., 2014; Schwarz et al., 2015, 2012). However, as the infiltration of the DECM by chondrocytes takes several weeks, the process has to be accelerated in order to prevent destabilization and degradation of the scaffold by inflammatory reactions in vivo.

Different dynamic culture (DC) systems have been developed to imitate physiologic biological and biochemical conditions within the

engineering process and thus to enhance the quality of the engineered cartilage (Concaro et al., 2009; Mabvuure et al., 2012).

As nutrient and oxygen supply of cartilage is based on diffusion, the transport of cytokines and chemokines into deeper tissue layers is limited and therefore hinders cellular migration. Likewise, the removal of catabolic products from the ECM is slow and as such is different from tissues with a distinct blood supply (Kellner et al., 2002; Zhou et al., 2008). In vivo several mechanical and chemical stimuli influence the transport of those substances which can be mimicked by dynamic cultures – so called bioreactors – to a certain extent.

As proven in former preliminary experiments, a bioreactor with continuous flow, that has been developed to optimize culture conditions to improve chondrogenic integrity and redifferentiation of these cells (Princz et al., 2016, 2017), was considered to facilitate cellular migration and support cellular re-differentiation. We thus examined the cultivation of DECM from porcine nasoseptal cartilage seeded with human nasal chondrocytes in this automated bioreactor for the purpose of cell migration and matrix production under standard normoxic conditions.

2 | MATERIALS AND METHODS

2.1 | Experimental bioreactor set-up

The bioreactor was engineered by the Department of Mechatronics and Medical Engineering, Ulm University of Applied Sciences. Its core is a double jacket glass vessel, which is heated to 37°C. It has connections for medium and gas inflow and outward flow, which can be automatically controlled by a custom-written control software on a separate PC. The detailed description of the system has been published previously (Princz et al., 2016, 2017). The medium inlet and outlet were positioned on opposite sides to achieve a homogenous, continuous flow. The cell-seeded surface of the DECM scaffolds was positioned vertically to the fluid flow. The cell layer was orientated against the incoming fluid flow. Overall, 18 DECM scaffolds were transfixed to three Kirschner wires of 0.6 mm diameter, that is six scaffolds to one wire, and set in the glass vessel where a continuous medium flow of 2 ml/min was applied by a peristaltic pump. The medium used was StemMACS ChondroDiff Media human (Miltenyi Biotec GmbH Bergisch Gladbach). Two-thirds of the total volume of the medium was changed twice a week by automatic medium exchange with a flow rate of 20 ml/min. The composition of the premixed gas (MTI IndustrieGase AG Neu-Ulm) was 5% CO₂, 20% O₂ and 75% N₂. One of the three wires with six DECM scaffolds each was removed after 14, 28 and 42 days of culture and analyzed as follows.

2.2 | Decellularized porcine cartilage matrix

DECM was obtained from fresh nasal septal cartilage from adult 7- to 8-month-old German landpigs from the local abattoir. Cartilage discs

without perichondrium with 5 mm in diameter and about 1 mm thickness were punched out and decellularized by a wet chemical process as has been previously described in detail (Schwarz et al., 2012, 2015). This procedure guarantees the removal of all immunogenic factors such as cells and GAGs. The samples were then lyophilized and dry stored until further use.

2.3 | Collection and amplification of human nasal septal chondrocytes

Human primary nasal chondrocytes (HPCH) were harvested from septal cartilage samples obtained during nasal surgery in the Department of Otorhinolaryngology, Head and Neck Surgery, Ulm University Medical Center. Informed Consent, approved by the University of Ulm Ethical Committee (Ethic application number 152/08), was signed by all five donor patients. The range of donors' age was 18–36 years, with an average of 28. HPCH were isolated according to standard protocols as formerly published (Goldberg-Bockhorn et al., 2018; Schwarz et al., 2012, 2015). Cells were pooled in order to obtain sufficient cell numbers and cryopreserved at -24°C until further use.

2.4 | Cell seeding and cultivation of DECM constructs in dynamic and static culture

Cryopreserved HPCH were initially thawed and amplified in monolayer culture for about 5 days until a confluence of 80%–90%. Only HPCH in passage two were used for the experiments. The lyophilized scaffolds were sterilized in 80% ethanol for 1 h, air dried under sterile conditions at room temperature (RT) and subsequently incubated in standard medium for 24 h at 37°C and 5% CO_2 to ensure rehydration and equilibration. Seeding was performed with 1×10^5 HPCH per scaffold. The scaffolds were placed in a 96-well plate (one scaffold per well). Cell suspension was pipetted onto each single scaffold and incubated for 5–6 h. Six prepared scaffolds were transfixed on a single Kirschner wire for DC and cultivated inside the bioreactor in a chondrocyte differentiation medium (NH ChondroDiff medium, Miltenyi) supplemented with 0.5% gentamicin. Scaffolds used as a static control were cultivated in a 12-well plate using the same medium. Medium exchange in static culture (SC) was performed twice a week (on Tuesday and Friday) by removing the old medium with pipettes and adding fresh medium in the same manner. Experimental analyses were conducted with six scaffolds in the DC and five scaffolds in the SC on days 14, 28 and 42 after seeding.

2.5 | Histological and immunohistochemical analyses

Morphology and distribution of the seeded chondrocytes were visualized by alcian blue staining counterstained with hematoxylin or

nuclear fast red. Specifically, it illustrates newly produced acidic sulfated GAG by an intensive blue staining. To enable several different methods of analysis, scaffolds were divided into three parts, one half and two quarters, for further analyses. One quarter of the DECM taken out from SC or DC was used for histological, immunohistochemical and TUNEL staining. It was fixed in 3.5%–3.7% neutral buffered formalin solution (Fischer) and embedded in paraffin. Tissue sections of 4 μm thickness from one cutting surface were generated and incubated at 56°C over night. The preparations were subsequently stained after deparaffinization and rehydration using a decreasing alcohol series, starting with xylol.

The immunohistochemical detection of newly synthesized aggrecan (ACAN), collagen type I (COL1A1) and COL2A1 was conducted by using EnVision+ System (Dako) according to the manufacturer's instructions. The primary antibody against ACAN (Millipore) was added to the deparaffined and dehydrated sections in a dilution of 1:100, the antibody against COL1A1 (Abcam) in a dilution of 1:800 and the antibody against COL2A1 (II-II6B3, Developmental Studies Hybridoma Bank) in a dilution of 1:400. The preparations were incubated for 1 h at RT in a humidified box, subsequently rinsed and incubated for further 30 min after adding the secondary antibody.

2.6 | Detection of apoptosis by colorimetric TUNEL assay

Slides with formalin fixed paraffin-embedded tissue sections (4 μm) from scaffolds cultivated either in DC ($n = 4$) or SC ($n = 4$) after 14, 28 and 42 days were deparaffinized and treated with proteinase K to permeabilize the tissues. The subsequent TUNEL Assay was performed using the DeadEnd Colorimetric TUNEL System – kit (Promega) according to manufacturer's instructions. Images with an objective lens of $20\times$ magnification of each TUNEL-stained section were made using an inverted transmitted light microscope (Axio Observer, Zeiss) equipped with an Axiocam 503 color camera (Zeiss) and the Zen 2.6 (blue edition) software (Zeiss). The total cell number and the number of TUNEL-positive (dark brown) cells were determined using ImageJ software (v1.52e). Three random fields per stained section, one from the edge, one from the center and one between center and edge, were analyzed. Results of all three fields from one section were summed up. Rates of dead cells were finally calculated.

2.7 | Computational analysis of the migration depth and cell numbers

Sections stained with alcian blue and nuclear fast red counterstaining were used for half-automated computational image analysis to determine the migration depth of the HPCH as well as the number of chondrocytes migrated into the scaffold (Figure 1). As cellular density on the scaffolds' surface was high and single cells could not be convincingly evaluated neither with the naked eye nor by the computer

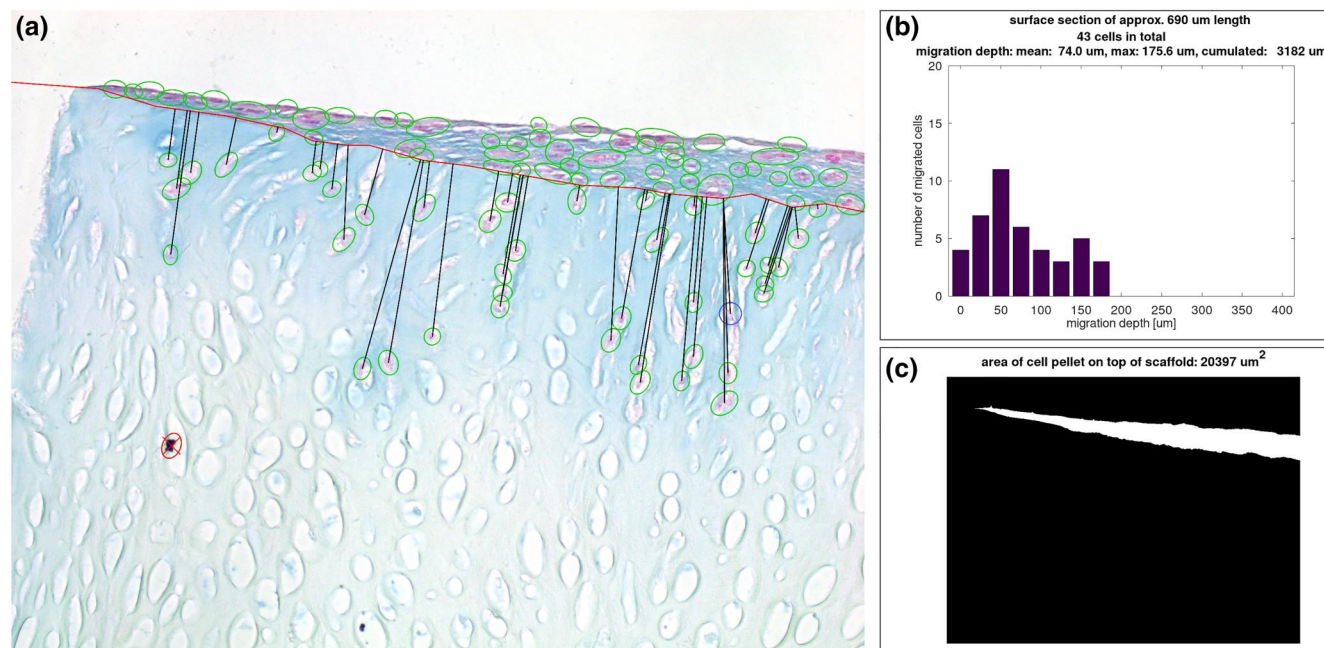


FIGURE 1 Computational analysis of microsections with alcian blue staining. (a) Exemplarily demonstrates the parameters of the computational analysis drawn in a picture from the center of a microscopic section of a scaffold cultured for 42 days in the bioreactor (named "BR Pos 5 42d center" in Figure 3). Human primary nasal chondrocytes (HPCH) marked with green circles were correctly detected by the computer program while cells marked with blue circles were added by the investigator. Cells marked with red circles and cross were incorrectly detected by the algorithm and were not included in the analysis. The black lines represent the shortest distance between the scaffold's surface (red line) and the migrated cells. Marked cells above the red line were not included in the calculations; (b) Indicates a histogram of the in (a) depicted section prepared in GNU Octave. It describes the number of migrated HPCH in relation to the migration depth. Further analyzed parameters are shown in the legend above the drawing. All histograms are summarized in Figure 3; (c) Depicts the automatically determined area of the cell pellet on the surface of the scaffold (white space) of the microscopic picture of (a) indicated in μm^2 [Colour figure can be viewed at [wileyonlinelibrary.com](https://onlinelibrary.wiley.com/doi/10.1002/jbm.b.3261)]

program, we determined and compared the area of accumulated cells consisting of all chondrocytes which settled and proliferated on top of the scaffold and did not migrate into it. This area of chondrocytes will be referred to as "cell pellet" in the following passages.

Stained sections were photographed using an inverted transmitted light microscope (Axio Observer, Zeiss) with 20 \times objective lens and the integrated camera AxioCam 503 color (Zeiss). Applied software was Zen 2.6 (blue edition). The image size was 1936 \times 1460 pixels. In order to examine differences between the peripheral area (edge) and the center of the scaffold, two images per scaffold were evaluated, one bordering to the edge of the scaffold and one bordering to the center point of the scaffold. The size of the region shown in each image was about 690 μm horizontally and about 520 μm vertically. A slight variance derived from the partly minor sloping of the sections within the pictures.

The image analysis was done using GNU Octave (v5.2.0) and is based on the idea behind Lepiarz et al. (2017). Programming sequence was as follows: The background in each image was subtracted and the image was linearly normalized to make the images comparable in terms of brightness and contrast. In a second step, cells were detected automatically using an adaptive thresholding procedure specifically adjusted to the images based on ratios of the RGB channels, for example. This was followed by morphological operations and filtering of the regions that were found in the previous

step for criteria like area and eccentricity. Next, the detected cells were marked in the image and presented to the user who had the opportunity to delete cells that were detected by mistake and/or add cells that were not identified by the algorithm. Afterwards, the user had to draw the boundary line in the image that separates the scaffold from the cell pellet. After finishing that, the migration depth of each migrated chondrocyte was calculated as the shortest distance to the boundary line, resulting in a list of migration depths per image. The migration depth per image was indicated as mean, maximum and cumulated migration depth. The latter represents the sum of migration depths of all migrated cells as a parameter of the infiltration of the scaffold and consequently its quality with regard to its implementation as tissue engineered cartilage. Additionally, the area of the cell pellet on top of the scaffold was determined by using the boundary line drawn by the user as lower boundary and again thresholding with different parameters for the upper boundary. Resulting pixels were counted and converted into μm^2 .

2.8 | Biochemical analyses

A second quarter of each scaffold was used for biochemical analyses. Direct measurement of sulfated GAG was performed using the dimethylmethylene blue (DMMB) assay as formerly published

(Schwarz et al., 2015) and described by Barbosa et al. (2003). Absorbance was measured at 656 nm. Determination of sulfated GAG was carried out by comparison with calibration curves of standard chondroitin sulfate solutions (data not shown).

The cell count per scaffold was indirectly measured using the QuantiFluor® dsDNA assay (Promega) according to the manufacturer's instructions. A calibration curve was generated with human nasal septal chondrocytes from the cell pool used. Fluorescence was measured in an Infinite M200 PRO microplate reader from Tecan at 504 nm_{Ex} and 550 nm_{Em}.

2.9 | Gene expression analysis

One half of each scaffold was used for gene expression analyses. De novo synthesis of COL1A1 and COL2A1 as well as ACAN was determined at gene expression level.

Scaffolds halves were removed from culture and snap-frozen afterwards. Homogenization was conducted in RLT-buffer (Qiagen, Hilden) with a tissue lyser (Qiagen) for 2 × 3 min at 50 Hz. According to the manufacturer's instructions (Qiagen), RNeasy Mini kit was used to isolate and purify RNA, including on-column DNase treatment. 200 ng of the total RNA were reversely transcribed with the QuantiTect Reverse Transcription Kit (Qiagen) and diluted 1:2 with RNase free water. Real-time PCR (rtPCR) was performed with 2 µl of each cDNA sample in duplicate in a LightCycler 96 (Roche). Table 1 gives an overview of the used primer and probes. Subsequently, denaturation passed at 95°C for 10 min followed by amplification in 45 cycles: 95°C for 10 s, followed by 60°C for 20 s and 72°C for 1 s. Measuring was performed after 14, 28 and 42 days in relation to the corresponding housekeeping gene glyceraldehyd-3-phosphate-dehydrogenase (GAPDH). Relative quantification of marker gene expression was calculated according to 2^{−ΔCt}, at which ΔCt = Ct of the target-Ct of the reference (Ct = cycle threshold).

2.10 | Statistical analyses

Results from the biochemical experiments, gene expression analysis and computational analysis were illustrated using GraphPad Prism

9.0.2 software (GraphPad Software). Scatter plots depict means and standard deviation (SD). Descriptive statistics and calculation of Pearson-r for correlations were also performed with GraphPad Prism 9.0.2 software. Mean with SD, median and range are indicated. Mann–Whitney test was conducted to examine statistical differences between center and edge regions before doing the descriptive statistics of the collective data. Regarding the small number of cases further statistical testing and the specification of a *p*-value were omitted.

3 | RESULTS

3.1 | Chondrocytes migrated deeper into the scaffolds in dynamic than in static culture

The evaluation of the histological preparations provided first information about cell migration and proliferation (Figure 2). The direction of migration was typically vertical to the scaffolds' surface in direction with the medium flow. However, if the orientation of the lacunae was more transvers to the surface – which was rarely the case – the HPCH followed this direction. Cells formed channels by connecting one lacuna to another. Migrating chondrocytes were followed by further cells in the channels building cell chains. Most cells were found on top of the scaffolds after the dynamic as well as the static cultivation. Very few cells settled on the sides or the bottom of the scaffolds and migrated only slightly from there following the orientation of the ECM and the lacunae. Cell proliferation was comparable on the top as well as on the sides of the scaffold. Migrating chondrocytes filled the lacunae and the nuclei were mostly round or oval. The cells, which built a layer on top of the scaffold, appeared flat and embedded in newly synthesized matrix. The nuclei were predominantly flat. The migration of the HPCH occurred homogenously across the entire scaffold.

The evaluation of the histological sections by our computational analysis showed no statistically significant differences between center and edge of the scaffolds for the parameters “number of migrated cells”, “cumulated migration depth” and “area of cell pellet” at any point of assessment, as illustrated in Figures 3 and 4 (*p* > 0.05).

The data show an increase of migrating HPCH from day 14 to day 42 in DC, while in SC the number of migrating cells increased until day 28 and decreased during proceeding cultivation (Figure 4b). Mean, SD,

TABLE 1 Primer and probes (Universal Probe Library, Roche) of the investigated genes used for real-time PCR

Gene	UPL probe	Primer left	Primer right
Target			
Collagen type I (COL1A1)	#15	5'-atgttcagctttgtggacctc-3'	5'-ctgtacgcaggtgattggtg-3'
Collagen type II (COL2A1)	#19	5'-ccctggtcttgggtggaac-3'	5'-tccttgcttactcccaactg-3'
Aggrecan (ACAN)	#79	5'-tgcagctgtcactgtagaaactt-3'	5'-atagcaggggatggtgagg-3'
Housekeeping			
GAPDH	#60	5'-gctctctgctcctctgttc-3'	5'-acgaccaaaccgttgactc-3'

Abbreviations: GAPDH, glyceraldehyd-3-phosphate-dehydrogenase.

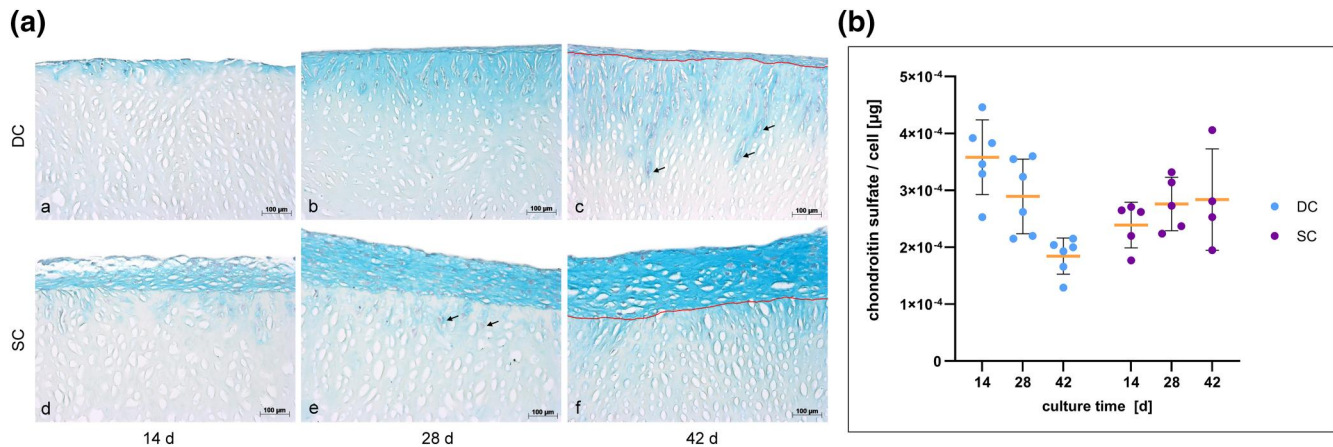


FIGURE 2 Histological staining and glycosaminoglycans (GAG) synthesis per cell verified by dimethylmethylene blue (DMMB) assay. (a) Results from alcian blue staining of histological sections at 14, 28 and 42 days. The upper row (a–c) shows the behavior of the chondrocytes in the dynamic culture (DC) in contrast to the static control (d–f). The red line in picture (c) and (f) depicts the border between the scaffold's surface and the chondrocytes on top of the scaffold. Newly synthesized GAGs are indicated by the blue coloring of the extracellular matrix around migrating and proliferating human primary nasal chondrocytes (HPCH). The cell layer on top of the scaffold is thicker in the static culture (SC) compared to the dynamic at all dates of examination. Nevertheless, migration of the chondrocytes into the scaffold is obviously enhanced in the bioreactor culture over time, while only a few cells penetrate the scaffold's surface in the static control. Black arrows highlight exemplarily chondrocytes which migrated into the scaffolds. The formation of tunnels during migration is remarkable; (b) Results from the DMMB assay of the scaffolds in DC ($n = 6$) showed a clearly higher synthesis of sulfated GAG at day 14 compared to the static control ($n = 5$). Yellow bars in the diagram depict mean with standard deviation. In the further course of the experiment GAG production diminished continuously in the DC until day 42, while the GAG content in the SC did not change significantly [Colour figure can be viewed at [wileyonlinelibrary.com](https://onlinelibrary.wiley.com/doi/10.1002/jbm.b.3261)]

median and range are depicted in Table 2. We noted that the number of migrated cells averaged over all scaffolds was 1.5 times higher in DC than in SC after 14 days, 2.5 times higher after 28 days and 5 times higher after 42 days. The cumulated migration depth averaged over all scaffolds was even more than 7 times higher in DC than in SC after 42 days. The maximum migration depth of cells in the DC ranged from 0 to 131 µm after 14 days, 69–384 µm after 28 days and 108–383 µm after 42 days. In SC the range was 0–142 µm versus 38–277 µm versus 33–257 µm. The variation of the cumulated depth of migration in both culture settings over time is presented in Figure 4c and Table 2. Figure 3 depicts the histograms of migration depths of all single evaluated images which demonstrate how many HPCH migrated which distance inside the scaffolds. It reveals that migration is mostly increasing between 14 and 28 days of cultivation in DC. In SC the increase of migration during proceeding cultivation is only marginal.

3.2 | Proliferation of chondrocytes increases during cultivation time

The analysis of the total cell count on the DECM with the Quanti-Fluor® assay showed a strong increase of cell numbers per scaffold during the cultivation for both dynamic and SC (Figure 4a and Table 3). It is remarkable that the averaged cell number of the scaffolds in DC was about the half of that of SC (2.9×10^5 vs. 5.8×10^5) after 14 days of cultivation. This difference, however, widely harmonized during proceeding cultivation.

Observing the histological preparations of the seeded scaffolds from the dynamic and static cultures stained with alcian blue, it

becomes immediately obvious that the number of chondrocytes on top of the DECM increased from date to date (Figure 2). This effect was much more evident in SC, where the cell layer was substantially thicker than in DC even after 14 days. The distribution of the HPCH settling and proliferating on the surface of the scaffolds was homogenously. The cells on top followed small irregularities of the scaffolds' surfaces. Seldomly found disruptions of the scaffold were filled with cells.

The microscopical observations were confirmed by the computational analysis of the area of the cell pellet on top of the scaffolds. The steep increase of the cell pellet in SC and the lower and slower proliferation in DC are illustrated in Figure 4d. Values of mean, median and range are presented in Table 2. The data disclose that despite the high cellular proliferation on top of the DECM in SC the HPCH did not migrate deeply into the matrix. Figure 4e demonstrates the relation between the increase of the cell pellet on the scaffolds' surfaces and the number of migrated cells. Pearson's correlation coefficient of "number of migrated cells" versus "cell pellet area" for DC and SC combined reveals a slight negative correlation (Pearson- $r = -0.369$, $p = 0.002$, 95% CI $[-0.56, -0.14]$). Calculated separately for "DC" and "SC" the analysis reveals an even lower correlation. For DC Pearson- r is 0.219 ($p = 0.199$, 95% CI $[-0.12, 0.51]$) and for SC Pearson- r is -0.014 ($p = 0.94$, 95% CI $[-0.37, 0.35]$).

3.3 | Synthesis of sulfated GAG is on a particularly high level in the first few days of dynamic cultivation

Unseeded or "blank" DECM typically does not stain with alcian blue as GAG are fully washed out during the decellularization process. In

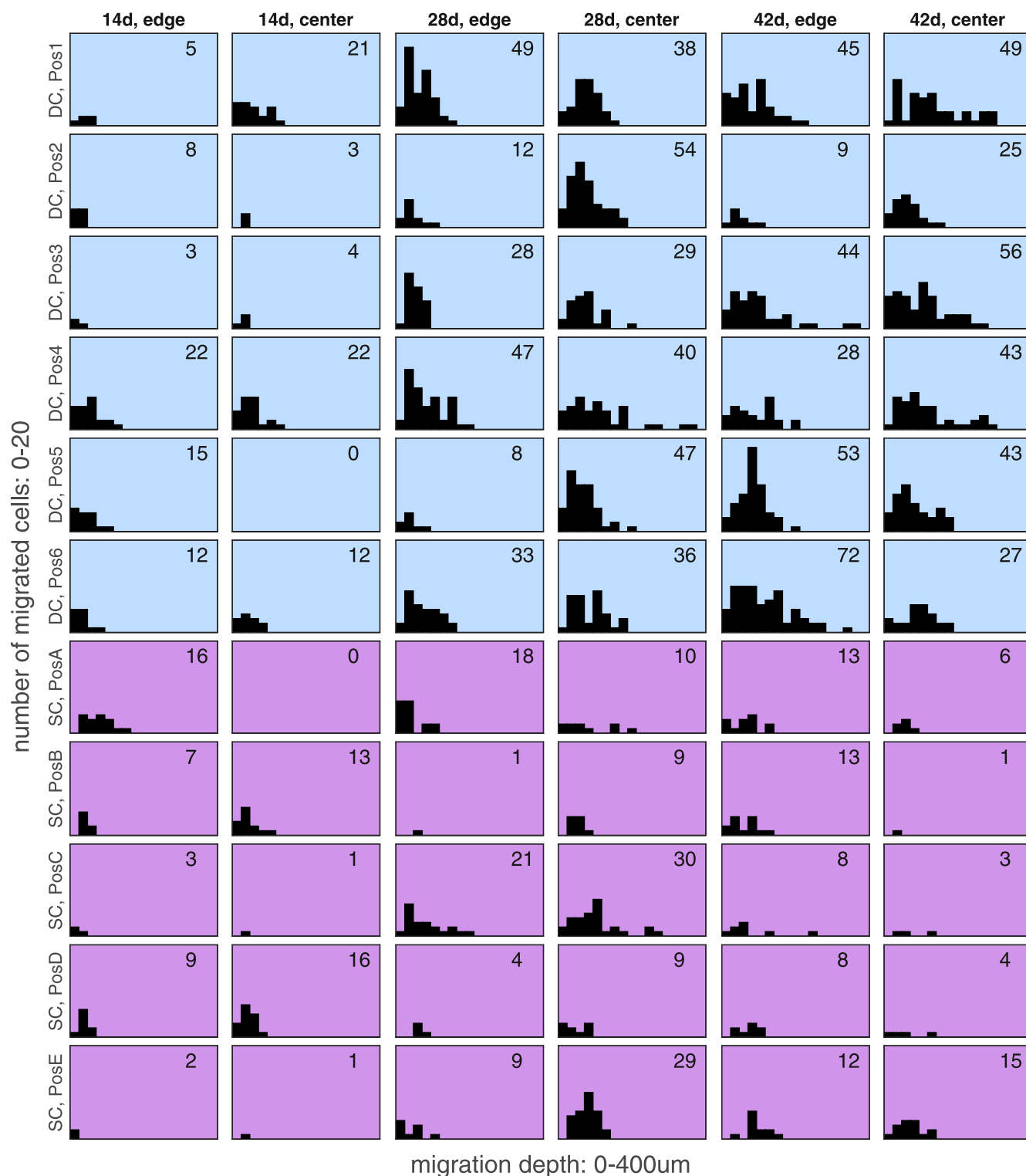


FIGURE 3 Histograms of the computational analysis concerning number of migrated HCPH and the migration depth of the cells. Analysis of two sections from each scaffold, edge and center, are outlined. “Pos1–6” indicate the position of the scaffold in the bioreactor (Pos 1 = nearest to the inflow of the medium, Pos6 = furthest away from the inflow of the medium). Histograms from the dynamic culture (DC) and static culture (SC) are presented in blue and violet, respectively. The number of the migrated cells counted in a single section is indicated in the respective histogram. The diagram exposes the increase of migrating cells during culture time, which was high in DC and low in SC. Migration depth increased homogenously which was consistent with the observations in the histological sections where human primary nasal chondrocytes (HPCH) formed tunnels and cell chains during migration. A high variance, but no clear tendency could be observed between sections from edge and center as well as regarding the position of the scaffold in the bioreactor [Colour figure can be viewed at [wileyonlinelibrary.com](https://onlinelibrary.wiley.com/doi/10.1002/jbm.b.3561)]

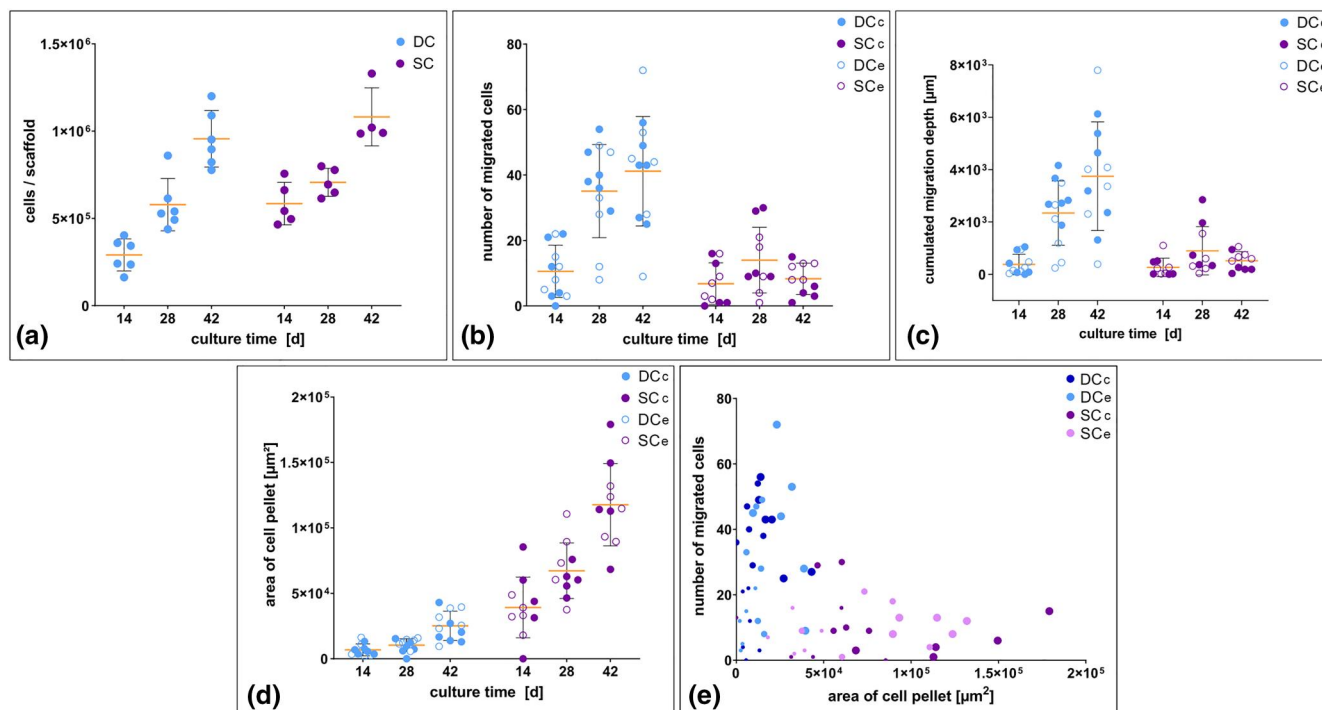


FIGURE 4 Scatter plots and bubble plot concerning cell proliferation and migration. The data is based on the QuantiFluor® assay (determination of cell numbers) (a) and the computational analysis (b–e). Yellow bars in the diagrams depict mean with standard deviation. (a) The graph illustrates an increase of the total cell numbers during the dynamic ($n = 6$) and static cultivation ($n = 5$). At day 14 considerably more cells settled on the scaffolds in the static culture (SC) compared to those in the dynamic culture (DC). This relevant difference vanished with proceeding culture time as cell numbers assimilated in both cultures; (b–d) Scatter plots in (b) reveal a strong increase of the number of cells migrating into the scaffolds in DC, while chondrocytes in SC migrated only very slightly; (c) The increasing number of migrating cells in DC went along with an increase of the cumulated migration depth; (d) In contrast, the area of the cells on top of the scaffolds increased stronger in SC than in DC; (e) The bubble plot illustrates the relation between the proliferation of the cell layer on top of the scaffolds and the number of migrated chondrocytes inside the matrix. Time of examination is depicted by the size of the bubbles (small = 14 days, middle = 28 days, big = 42 days). SCc center region in SC, SCe edge region in SC [Colour figure can be viewed at [wileyonlinelibrary.com](https://onlinelibrary.wiley.com/doi/10.1002/jbm.b.3261)]

TABLE 2 Descriptive statistics of the parameters collected in the computational analysis

	Number of migrated cells					Cumulated migration depth ($\times 10^2 \mu\text{m}$)					Area of cell pellet ($\times 10^3 \mu\text{m}^2$)				
	Mean	SD	Median	Min	Max	Mean	SD	Median	Min	Max	Mean	SD	Median	Min	Max
DC^a															
14 days	10.58	7.98	10.00	0.00	22.00	3.78	3.90	2.04	0.00	10.48	6.81	4.51	5.64	1.95	16.30
28 days	35.08	14.23	37.00	8.00	54.00	23.39	12.28	26.63	2.45	41.63	10.39	4.81	11.84	0.00	15.89
42 days	41.17	16.71	43.50	9.00	72.00	37.47	20.76	36.86	3.87	77.96	25.17	11.19	24.35	9.52	43.04
SC^b															
14 days	6.80	6.36	5.00	0.00	16.0	2.67	3.52	1.33	0.00	11.02	39.19	23.16	36.08	0.00	85.45
28 days	14.00	10.03	9.50	1.00	30.0	8.98	9.21	4.84	0.38	28.49	67.24	21.21	61.65	37.49	110.60
42 days	8.30	4.81	8.00	1.00	15.0	5.20	3.44	5.52	0.33	10.56	117.71	31.43	114.45	68.37	179.09

Abbreviations: DC, dynamic culture; SC, static culture; SD, standard deviation.

^aDynamic cultivation.

^bStatic cultivation.

contrast, alcian blue staining from seeded scaffolds cultured in the bioreactor as well as in SC showed a strong blue coloration around the chondrocytes on top and inside the scaffolds during the whole cultivation time, indicating a de novo synthesis of GAG (Figure 2a–f). A

differentiation between the synthesis wcapability of the superficially settled and the migrating cells was not possible with this method.

The positive GAG synthesis of the chondrocytes was verified and quantified by the DMMB assay (Figure 2g). Data demonstrate a

TABLE 3 Descriptive statistics of the biochemical analysis of the total cell numbers per scaffold (Quantifluor® dsDNA assay) and the content of chondroitin sulfate per cell and scaffold (DMMB Assay)

	Cells/scaffold ($\times 10^5$)					Chondroitin sulfate (GAG)/cell ($\times 10^{-4}$ μg)					Chondroitin sulfate (GAG)/scaffold ($\times 10^2$ μg)				
	Mean	SD	Median	Min	Max	Mean	SD	Median	Min	Max	Mean	SD	Median	Min	Max
DC ^a															
14 days	2.91	0.92	2.92	1.62	4.03	3.58	0.66	3.65	2.53	4.46	1.02	0.31	0.96	0.63	1.53
28 days	5.80	1.50	5.34	4.38	8.60	2.89	0.66	2.93	2.15	3.60	1.62	0.30	1.69	1.14	1.91
42 days	9.56	1.62	9.24	7.77	12.00	1.85	0.32	1.97	1.29	2.15	1.75	0.35	1.86	1.16	2.11
SC ^b															
14 days	5.84	1.22	5.43	4.65	7.56	2.39	0.40	2.62	1.77	2.71	1.37	0.26	1.34	1.09	1.76
28 days	7.06	0.80	6.94	6.14	7.99	2.76	0.47	2.73	2.24	3.32	1.92	0.15	1.90	1.74	2.15
42 days	10.81	1.66	10.05	9.86	13.30	2.84	0.89	2.67	1.95	4.06	3.05	0.93	3.08	1.92	4.12

Abbreviations: DC, dynamic culture; DMMB, dimethylmethylene blue; GAG, glycosaminoglycans; SC, static culture; SD, standard deviation.

^aDynamic cultivation.

^bStatic cultivation.

significantly higher expression of GAG per cell in the bioreactor culture compared to the SC after 14 days. Table 3 indicates mean, median and range of GAG synthesis per cell in detail. While chondrocytes in SC produced stable amounts of GAG during the further cultivation period, production of GAG strongly decreased from day 14 to day 42 in DC. This decline led to a bisection of GAG synthesis per cell within 4 weeks of cultivation (mean 3.6×10^{-4} vs. 1.9×10^{-4} , median 3.7×10^{-4} vs. 2.0×10^{-4}). However, the total GAG content per scaffold increased in both cultures during the cultivation. Mean values rose in DC from 101.65 ± 31.11 μg on day 14 to 175.20 ± 34.91 μg on day 42. In SC mean value clearly increased from 137.36 ± 25.59 μg after 14 days of cultivation to 305.18 ± 93.08 μg after 42 days.

3.4 | Collagen II expression decreases in dynamic and increases in static culture conditions

Immunohistochemical staining showed a comparable positive detection of ACAN as well as COL1A1 in the HPCH which were seeded onto the scaffold in both cultures, static and dynamic (Figure 5a). Collagen type II synthesis was much more pronounced in the HPCH in SC, while it was nearly absent in DC. Aggrecan and COL1A1 were synthesized by chondrocytes in the cell layer on top of the scaffolds as well as by those migrating into deeper ECM layers. In Figure 5i,m a delicate staining of COL1A1 is visible around the migrating cells and in the cytoplasm of the cells demonstrating the synthesis of new proteins by the migrating HPCH.

Real-time tPCR widely confirmed our results from the immunohistochemical stainings (Figure 5b and Table 4). With regard to the ACAN expression we detected a definitively higher relative ratio (ACAN/GAPDH) in DC at day 14 compared to SC. While ACAN expression relevantly decreased from day 14 to 42 in the bioreactor

culture, a sharp increase occurred in the SC. After 28 days ACAN expression was significantly lower in DC compared to SC. This development remained stable until day 42. As already shown by immunohistochemistry, the quantification of COL2A1 expression as a marker for redifferentiation confirmed the very low COL2A1 synthesis in the bioreactor system at day 42 in contrast to the high production of COL2A1 by chondrocytes in the SC. Collagen type II expression was at the same low level after 14 days in both cultures and showed no relevant difference. During further cultivation COL2A1 expression gradually decreased in DC and increased in SC. In contrast to the ACAN and COL2A1 expression the synthesis of COL1A1 doubled from day 14 to day 42 in DC while it remained widely stable in SC. Mean values, median and ranges are presented in detail in Table 4.

3.5 | Increase of cell apoptosis is stronger in static than in dynamic cultivation

To assess the viability of the cells in and on the DECM during cultivation, a TUNEL assay was performed. Our results reveal that the mean rate of apoptosis seems to be lower in samples in DC compared to samples in SC at all three examined times (Figure 6). While apoptosis rates of cells of the examined scaffolds in DC were relatively homogeneous, the range of the samples in SC varied widely, especially on day 28 and on day 42.

4 | DISCUSSION

Migration of cells into a scaffold and production of newly synthesized matrix proteins is a prerequisite to obtain cartilage in vitro. The interaction between cells and ECM require those morphodynamic

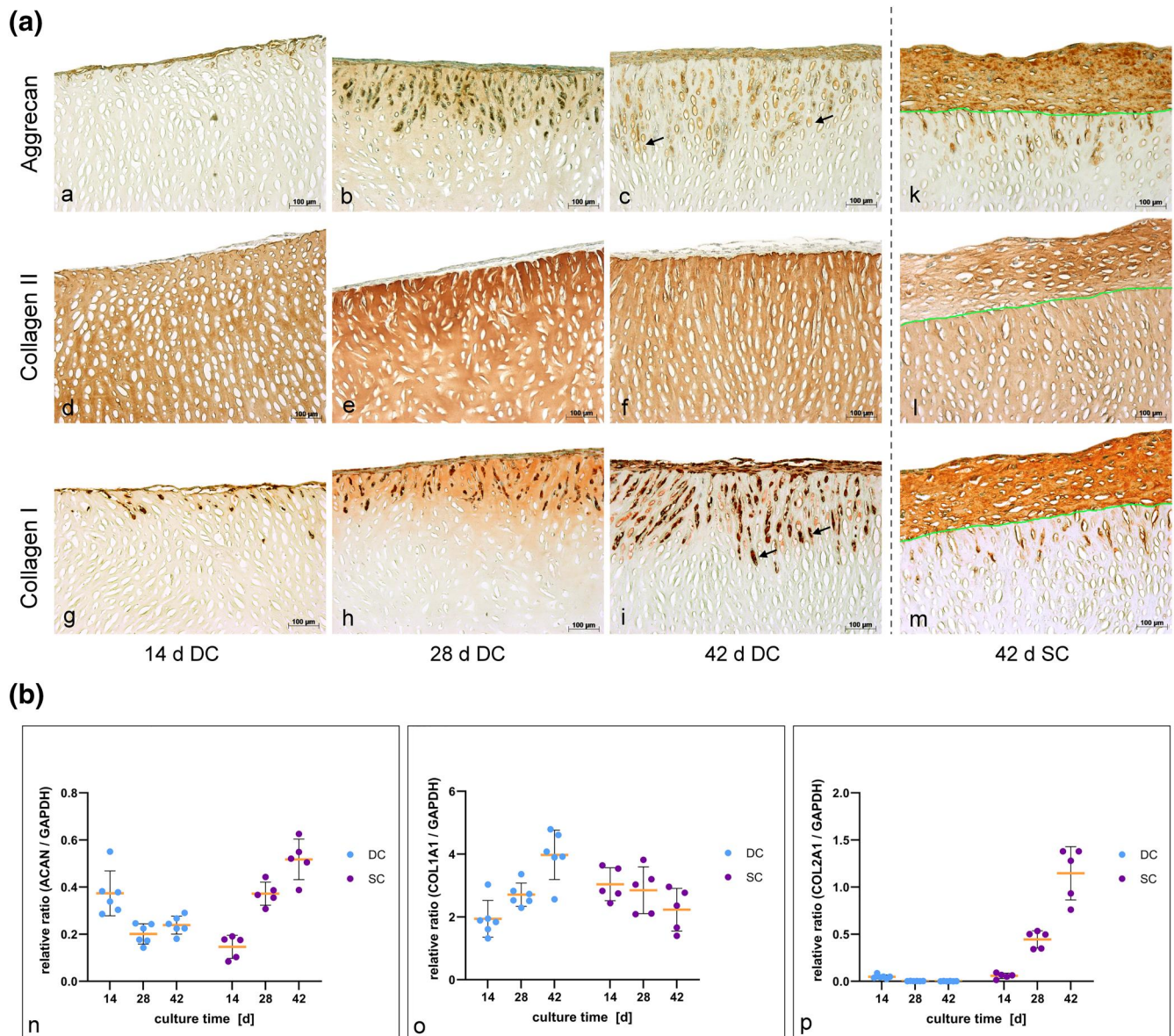


FIGURE 5 Detection of newly synthesized matrix by immunohistochemical staining and gene expression analysis. (a) Microsections from the dynamic culture (DC) with immunohistochemical staining are depicted in comparison to the static control. The green lines in the microsections from the static culture (SC) (k-m) indicate the border between the scaffold and the chondrocytes on top. Pictures (a-c) and (k) reveal a positive aggrecan (ACAN) synthesis of the cells (brown coloring, black arrow in c exemplarily) during the course of the experiment. While synthesis of new collagen type II (COL2A1) (d-f and l) was only marginal in the DC, it was clearly visible in the control sections (brown coloring of the cell cluster on top of the scaffold). Chondrocytes showed a positive synthesis of COL1A1 during proliferation as well as migration (g-i and m), which is indicated by the brown coloring of the cells on top and inside the decellularized porcine cartilage matrix (DECM) (black arrow in [i] exemplarily). The synthesis of new COL1A1 by migrating HCPH is indicated by a slight staining around the cells inside the scaffold (i and m). As porcine nasal septal cartilage nearly solely consists of COL2A1, which is evident in the COL2A1 staining (d-f and l; brown coloring of the scaffolds' matrix), the scaffold is nearly lucent after COL1A1 staining (g-i and m); (b) Real time-PCR analysis of ACAN (n), COL1A1 (o) and COL2A1 (p) expression demonstrates a clearly higher ACAN synthesis and obviously lower COL1A1 synthesis in DC after 14 days of cultivation compared to SC. COL2A1 was expressed on a comparable level at this date. Continuing cultivation induced a significant decrease of ACAN and COL2A1 production in the DC until day 42. In contrast, COL1A1 expression was apparently rising, demonstrating a proceeding dedifferentiation of the chondrocytes in DC. The static control, however, showed a significant increase of ACAN and COL2A1 expression, while COL1A1 synthesis showed a slight decrease [Colour figure can be viewed at [wileyonlinelibrary.com](https://onlinelibrary.wiley.com/doi/10.1002/jbm.b.35261)]

processes (Yamada & Sixt, 2019). Thereby, intrinsic and extrinsic factors influence the mode, success and speed of migration. As intrinsic factors like expression of genes or the condition of signaling

depend on the specific cell type, extrinsic factors mean the properties of the cellular environment. The latter include, for instance, the presence of adjoining cells, the composition of the ECM, the stiffness

TABLE 4 Descriptive statistics of the rtPCR data. Genexpression is given in relation to the housekeeping gene GAPDH

	ACAN/GAPDH					COL1A1/GAPDH					COL2A1/GAPDH ($\times 10^{-2}$)				
	Mean	SD	Median	Min	Max	Mean	SD	Median	Min	Max	Mean	SD	Median	Min	Max
DC^a															
14 days	0.37	0.10	0.36	0.29	0.55	1.94	0.58	1.87	1.32	3.03	4.85	2.04	4.56	2.62	8.63
28 days	0.20	0.04	0.20	0.14	0.25	2.71	0.37	2.63	2.29	3.36	0.30	0.10	0.30	0.17	0.43
42 days	0.24	0.04	0.23	0.18	0.29	3.98	0.79	4.00	2.56	4.79	0.20	0.08	0.15	0.13	0.31
SC^b															
14 days	0.15	0.05	0.18	0.08	0.19	3.04	0.52	2.83	2.44	3.64	5.81	2.82	6.36	1.55	9.25
28 days	0.37	0.05	0.37	0.31	0.44	2.85	0.75	3.03	2.09	3.82	44.48	9.18	49.70	34.20	53.40
42 days	0.52	0.09	0.52	0.39	0.63	2.23	0.68	2.36	1.40	2.96	114.68	28.33	128.00	76.10	138.00

Abbreviations: ACAN, aggrecan; COL1A1, collagen type I; COL2A1, collagen type II; DC, dynamic culture; GAPDH, glycerinaldehyd-3-phosphate-dehydrogenase; rtPCR, real-time PCR; SC, static culture; SD, standard deviation.

^aDynamic cultivation.

^bStatic cultivation.

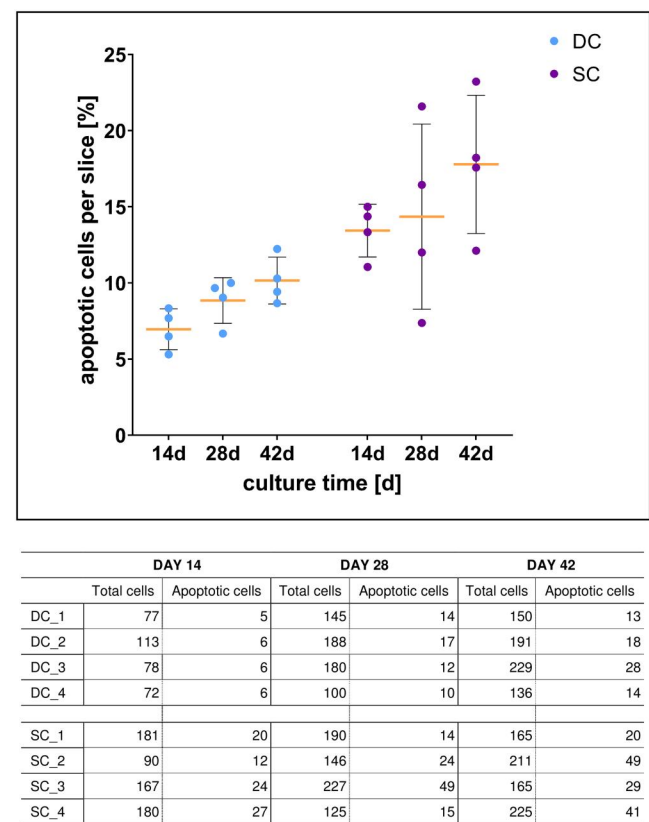


FIGURE 6 Cell viability during cultivation. Scatter plot demonstrates the rates of apoptotic chondrocytes, which were calculated from the TUNEL assay data of four histological sections each from dynamic (DC) and static culture (SC). Yellow bars depict mean with standard deviation. The corresponding table shows cell numbers summarized from the counting of three random fields of each analyzed section [Colour figure can be viewed at [wileyonlinelibrary.com](https://onlinelibrary.wiley.com)]

of the material and the pore size. Those factors can be very challenging for migrating cells. Preexisting pores and tunnels can facilitate and accelerate migration, whereas dense and stiff fiber networks

may require greater efforts and the need to change the mode of migration (Yamada & Sixt, 2019).

A positive effect of the dynamic cultivation is the improved migration of the cells inside the scaffold in comparison with our static cultivation. Our experiments revealed that the total amount of cells on the scaffolds in DC was the half of the number of cells in SC after 14 days of cultivation. The percentage of migrating HPCH was approximately the same at this time in both cultures. Consequently, the cell layer on top of the scaffold was thicker in SC than in DC. This difference may have been caused by the fact that the scaffolds had to be handled in order to put them on the Kirschner wires after the seeding process, so that cells may have become detached. Subsequent horizontal cultivation in the medium flow may then have caused cells, which were not yet firmly adherent to the scaffold, to float away. With proceeding cultivation, the total amount of HPCH adjusted between the cultures. While the chondrocytes on the scaffolds in SC proliferated on top of the DECM, the cells in DC proliferated and migrated at once. Consequently, the increase of apoptotic HPCH was stronger in SC than in DC, probably due to the decreasing nutrient and oxygen supply in the growing, dense cell layer on top of the DECM (Figure 6). These differences in proliferation and migration may arise from two different factors: the total number of cells on the scaffolds at the start of cultivation – that we could not definitely determine – and the mechanical forces of the medium flow in DC. Before observing our data, one might assume that a thicker cell pellet on the scaffold would lead to a more pronounced migration of cells into the scaffold. Figure 4e disproves this assumption, however. Accordingly, the Pearson's correlation coefficient for DC and SC combined even reveals a slight negative correlation. This negative correlation is probably not based on a causal relationship between the two examined parameters, but is caused by the “confounder” cultivation method. The medium flow might be hypothesized as an important variable. This becomes clear when calculating the correlation coefficient for DC and SC separately to avoid the influence of the confounder. As the correlation of the isolated groups is even

smaller and differs in leading sign, one can conclude that the thickness of the cell pellet on top of the scaffold has no influence on the migration of the cells.

Furthermore, the difference in cultivation – horizontal versus vertical – may influence the distribution of the cells on the scaffold as gravity acts on the cells in two different directions and may lead to an accumulation of cells in the lower zones of the scaffold in the vertical DC in contrast to a homogeneous distribution in the horizontal SC. It might be argued, if gravity would have a major influence on the migration process, HPCH in SC would have migrated much easier and deeper into the scaffold than in DC, however. Even though we did not observe obvious variations in the cells' distribution in our samples, the probable influence of gravity on differentiation and migration has to be considered and examined in further studies. The number of migrating cells and the depth of migration of these cells are both characteristics of a high-quality migration process in our opinion. The difference in the migration depth between the static and DC is particularly obvious after 28 and 42 days of cultivation (Figures 2a–f, 3, and 4c). As is generally known, a high density and compact network of collagen fibers slows down the already slow mesenchymal migration process (Yamada & Sixt, 2019). Although the decellularized matrix, whose collagen network is close to the natural hyaline cartilage, has distinct advantages with regard to stability, the porosity of the material seems to have clear limitations concerning migration of the cells (Schwarz et al., 2012, 2015). It is known from studies of human nasal cartilage that the orientation and the shape of the lacunae as well as the density of collagen vary between peripheral and central zones of the cartilage (Popko et al., 2007). Although we only use the central zones of the porcine cartilage for preparing the DECM scaffolds, we noticed a large variety in the density of the collagen framework. The influence of the pore size on migration was demonstrated in several studies (Luo et al., 2015; Rowland et al., 2016). The forming of tunnels by ECM remodeling through the secretion of proteolytic enzymes, as seen in the histological preparations, is characteristic to the mesenchymal migration process, but is typically very slow (Yamada & Sixt, 2019). Cell–cell and cell–ECM interactions enable thereby other cells to follow and move forward through such generated tunnels (Gaggioli et al., 2007). The chondrocytes seem to require the mechanical stimulus of the continuous medium flow to switch from proliferation and differentiation to migration into the dense collagen matrix. However, cells did not completely permeate the scaffold in the bioreactor, even not after 42 days of cultivation.

Oxygen and nutrient supply may therefore play a supporting role aside from mechanical and geometrical factors (Magliaro et al., 2019). Kellner et al. (2002) examined the oxygen distribution in natural and engineered cartilage discs and found decreasing gradients of oxygen in both tissues. They discussed the influence of several factors on the oxygen distribution and consumption as cell density and growth, oxygen demand of developing and mature tissue as well as the different or rather changing density of the ECM. Similar to our study, they observed a limited tissue development and cell migration into the scaffolds and explained this with the decreasing oxygen pressure in deeper tissue layers. In addition, Zhou et al. (2008) pointed out

that oxygen demand and consumption depend not only on the oxygen concentration, but also on the nutrient supply and pH.

It is suspected that the motility and flexibility of cells improve the more physiological the ECM is (Yamada & Sixt, 2019). A main problem of common in vitro cultures of three-dimensional cartilage scaffolds is the lack of an adequate culture environment mimicking the natural physicochemical and mechanical characteristics which exist in vivo. In this context, different bioreactors have been developed to imitate some of these natural conditions. It has to be considered that most of the described bioreactors are not fully comparable with our glass reactor. Perfusion flow bioreactors are probably the most comparable reactors. However, in perfusion flow bioreactors the medium is continuously forced through the scaffold and does not circulate around it, so that shear stresses will be relatively high (Concaro et al., 2009; Mabvuure et al., 2012). In contrast, in our bioreactor the scaffolds are surrounded and flushed by medium with the lowest flow rate that was technically possible with the peristaltic pump used. As verified in different computational simulations, the level of medium flow plays a role in the differentiation and proliferation of cells in such dynamic cultures (Devarapalli et al., 2009; Pierre et al., 2008; Shahin & Doran, 2011). Wall shear stresses induced by the medium flow, which may affect each cell in bioreactors, depend on the composition of the scaffold and can induce a change in protein synthesis. In the bioreactor used in this study the disk-like scaffolds were vertically positioned and oriented with the cell-seeded side towards the incoming medium flow. Wall shear stresses are therefore higher on the cell-seeded side, highest on the scaffold in the position nearest to the medium inflow and higher on the edges of the scaffolds than in the center. Even though the position of the scaffolds in the bioreactor used does not seem to make any difference concerning the migration of the HPCH in our study (Figure 3), the amount of shear stresses may be an influencing factor in dynamic cultures. Indeed, the amount of shear stresses can be regulated by the flow rate (Concaro et al., 2009). The discussion on this topic is partly contradictory. Flow rates between 0.05 and 0.1 ml/min and below seem to have advantages over higher flow rates, because especially in the beginning of the culture high flow rates can remove cells from the scaffold (Concaro et al., 2009) and lower flow rates are supposed to be more efficient with regard to matrix synthesis (Khan et al., 2009). However, increasing the flow rate after some days of cultivation with low rates may lead to an increase of cell content, DNA and GAG synthesis (Davisson et al., 2002). Compared to other types of bioreactors flow perfusion reactors came up to a better nutrient supply inside three-dimensional scaffolds and led to a higher GAG synthesis than in the common static cultivation (Mabvuure et al., 2012). However, continuous flow reactors with very low flow rates are still more efficient and profitable concerning ECM production (Khan et al., 2009). In our current study the production of GAG and the expression rates of ACAN were significantly higher in the bioreactor culture on day 14 compared to the static control, while COL1A1 expression was significantly lower and COL2A1 expression was comparable to static controls. Whereas a differentiated chondrocyte is characterized by the expression of COL2A1 and ACAN, which gets lost during the dedifferentiation process in monolayer culture (Hamada et al., 2013), the

synthesis of COL1A1 is a typical attribute of a dedifferentiated chondrocyte with a fibroblastic phenotype (Caron et al., 2012). Our results therefore reveal a better re-differentiation of cells under dynamic cultivation compared to SC conditions, at least after 14 days. The outcome was even better than in other studies with perfusion reactors or under continuous flow (Khan et al., 2009; Tonnarelli et al., 2016). That seems to indicate that our continuous laminar flow culture with a flow rate of 2 ml/min might have some advantages in the first 14 days of cultivation even though or just because our setup has 20 times higher flow rates than other continuous flow reactors (Khan et al., 2009).

Nevertheless, further dynamic cultivation showed proceeding negative effects on the cells' differentiation – as depicted by our DMMB and rtPCR data (Figures 2g and 5) – in contrast to the static cultivation. This could just as well be a consequence of the fixed medium flow rate but also of the limitation of nutrient and oxygen supply in deeper tissue layers as discussed before. Therefore, the adaption of the flow rate in our bioreactor after 14 days of cultivation could possibly lead to a sustained differentiation of the cells. Whether higher or lower flow rates are more promising and how they may influence the migration of HPCH, has to be verified in further studies. Concluding our results, we revealed two different patterns of behavior in the cultures. During static cultivation chondrocytes exhibited a high proliferation rate and redifferentiated by up-regulating the gene expression of specific collagens and characteristic matrix proteins (increase of ACAN and COL2A1 expression, stable GAG synthesis and decrease of COL1A1 expression after 28 days). In the bioreactor culture, however, the cells also proliferated, and differentiation was superior compared to the SC after 14 days (significantly higher rates of GAG synthesis per cell and ACAN expression, similar rates of COL2A1 expression, lowest rates of COL1A1 expression). In the further course of cultivation, the migration of the chondrocytes into the scaffold was forced by the medium flow, and simultaneously the differentiation of the cells was increasingly lost. With respect to the literature, it seems obvious that differentiation comes at the expense of migration. It is known from studies of chondrogenic progenitor cells, which have stem cell like properties with a high chondrogenic potential (Jiang et al., 2016; Koelling et al., 2009) and are therefore less differentiated than mature chondrocytes (Elsaesser et al., 2016; Koelling et al., 2009), that their migration properties are superior to those of mature chondrocytes. This is supposed to be due to the higher expression of matrix metalloproteinases (MMP) and other ECM-degrading enzymes (Elsaesser et al., 2016; Koelling et al., 2009). The role of MMPs in cell migration is very complex and – concerning our experimental setup – has to be examined in further experiments.

A limiting point of our studies is that the morphology of the HPCH cannot be fully determined by the histological staining. As migration induces morphologic changes in the cytoskeleton and the nucleus, like the formation of lamellipodia, the organization of microtubules and nuclear deformation (Yamada & Sixt, 2019), scanning electron microscopy and transmission electron microscopy as well as fluorescence microscopy could probably elucidate those alterations

and offer valuable cues to the mode of migration, potential problems or inhibiting factors. Furthermore, the site of matrix production (on top or inside the scaffold) could not exactly be located by biochemical or gene expression analysis. That is why we cannot prove our hypothesis that cells can either migrate at the expense of differentiation or concentrate on proliferation and matrix production. Besides, we did not measure the nutrient and oxygen supply inside the scaffold and therefore could not analyze a potential decrease in the supply as a possible reason for the increasing dedifferentiation while the migration increases during the cultivation. At last, the scaffolds in the bioreactor were cultivated vertically in contrast to the horizontal cultivation in SC. Therefore, gravity may have influenced the distribution and migration of the chondrocytes on top of the scaffolds as mentioned above, even though we did not explicitly observe this in our histological sections. Vertical cultivation of the static preparations could be a solution in future experiments to establish better comparability. With regard to the many influencing factors, experiments with a larger number of samples would provide an even higher grade of statistical evidence.

In conclusion, our experiments revealed the potential of HPCH to migrate into the DECM, if cultivated in the continuous laminar flow bioreactor, despite the relatively dense collagen network of the scaffolds. The loss of differentiation capacity during cultivation may be a fact of genetic re-programming as cells may activate migration and the production of ECM-degrading factors at the expense of chondrogenic differentiation. This hypothesis has to be confirmed by further experiments, for example the determination of ECM-degrading proteins such as MMP. Future strategies could include optimizing the cell seeding process to enable more chondrocytes to adhere to the scaffolds' surface. In addition, the medium flow has to be regulated to maintain a balance between a stronger fixation of the cells on top of the scaffolds and the adequate mechanical stimuli to facilitate and further optimize cell migration. The analysis of the amount of de novo synthesized proteins in the consumed medium, which have been washed out by the continuous medium flow before the integration into the ECM, would also be a helpful parameter to determine the optimal flow rate. As migration of the chondrocytes was strongest in the first two to four weeks a subsequent reduction of the medium flow might enhance gene expression and cell differentiation. Furthermore, the behavior of the chondrocytes under hypoxic conditions might have a positive influence on chondrogenic differentiation and matrix synthesis, as has been demonstrated in other studies before (Coyle et al., 2009; Daly et al., 2018).

Those additional experiments will further help to elucidate the complex interactions between cells and ECM in the future. The cultivation in the custom-made glass-vessel bioreactor presents a promising tool to support these efforts.

ACKNOWLEDGMENTS

The authors thank Katja Hasch for her dedicated, excellent work on the project and Gabriela Cudek for her technical support in the research laboratory. In addition, we thank Dr. biol. Ludwig Körber and Dr. rer. nat. Roman Breiter from the Institute of Bioprocess

Engineering, Erlangen University, who fabricated the porcine cartilage scaffolds and assisted with the realization of some experiments.

Open Access funding enabled and organized by Projekt DEAL.

CONFLICT OF INTEREST

The authors have no financial conflicts of interest. Funding was provided by the Federal Ministry of Education and Research (BMBF, funding reference number #03FH00813) as part of the "BioopTiss" project.

AUTHOR CONTRIBUTION

Prof. Dr. Nicole Rotter and Prof. Dr. Martin Hessling devised the project and the main conceptual ideas. They were both mainly involved in critically revising the manuscript and gave final approval of the manuscript to be published. The focus of Prof. Rotter was on the experimental laboratory part and the focus of Prof. Hessling on the technical part concerning the bioreactor. Dr. Eva Goldberg-Bockhorn and Dipl. Ing. (FH) Ulla Wenzel mainly performed the experiments, evaluated and interpreted the results and drafted the manuscript and figures. Dr. Marie-Nicole Theodoraki and Dr. Johannes Doescher statistically evaluated the data and supported the final interpretation. Dr. Ricarda Riepl, Dr. Marlene C. Wigand, Prof. Dr. Cornelia Brunner, Dipl.-Ing. Johann Kern and Prof. Dr. Thomas Hoffmann supported the evaluation of the results. They critically revised and worked on the manuscript regarding their individual focus.

DATA AVAILABILITY STATEMENT

The data that support the findings of this study are available from the corresponding author upon reasonable request.

ORCID

Eva Goldberg-Bockhorn  <https://orcid.org/0000-0001-5431-7458>

REFERENCES

- Barbosa, I., Garcia, S., Barbier-Chassefière, V., Caruelle, J.-P., Martelly, I., & Papy-García, D. (2003). Improved and simple micro assay for sulfated glycosaminoglycans quantification in biological extracts and its use in skin and muscle tissue studies. *Glycobiology*, 13(9), 647–653. <https://doi.org/10.1093/glycob/cwg082>
- Benders, K. E. M., van Weeren, P. R., Badylak, S. F., Saris, D. B. F., Dhert, W. J. A., & Malda, J. (2013). Extracellular matrix scaffolds for cartilage and bone regeneration. *Trends in Biotechnology*, 31(3), 169–176. <https://doi.org/10.1016/j.tibtech.2012.12.004>
- Berghaus, A. (2007). Implants for reconstructive surgery of the nose and ears. *GMS Current Topics in Otorhinolaryngology, Head and Neck Surgery*, 6, Doc06. <http://www.ncbi.nlm.nih.gov/pubmed/22073082>
- Bos, E. J., Pluemeekers, M., Helder, M., Kuzmin, N., van der Laan, K., Groot, M.-L., van Osch, G., & van Zuijlen, P. (2018). Structural and mechanical comparison of human ear, alar, and septal cartilage. *Plastic and Reconstructive Surgery-Global Open*, 6(1), e1610. <https://doi.org/10.1097/GOX.0000000000001610>
- Caron, M. M. J., Emans, P. J., Coolen, M. M. E., Voss, L., Surtel, D. A. M., Cremers, A., van Rhijn, L. W., & Welting, T. J. M. (2012). Redifferentiation of dedifferentiated human articular chondrocytes: Comparison of 2D and 3D cultures. *Osteoarthritis and Cartilage*, 20, 1170–1178. <https://doi.org/10.1016/j.joca.2012.06.016>
- Chiu, L. L. Y., Giardini-Rosa, R., Weber, J. F., Cushing, S. L., & Waldman, S. D. (2017). Comparisons of auricular cartilage tissues from different species. *Annals of Otology, Rhinology & Laryngology*, 126(12), 819–828. <https://doi.org/10.1177/0003489417738789>
- Concaro, S., Gustavson, F., & Gatenholm, P. (2009). *Bioreactors for tissue engineering of cartilage* (pp. 125–143). Springer. https://doi.org/10.1007/978-3-540-69357-4_6
- Coyle, C. H., Izzo, N. J., & Chu, C. R. (2009). Sustained hypoxia enhances chondrocyte matrix synthesis. *Journal of Orthopaedic Research*, 27(6), 793–799. <https://doi.org/10.1002/jor.20816>
- Daly, A. C., Sathy, B. N., & Kelly, D. J. (2018). Engineering large cartilage tissues using dynamic bioreactor culture at defined oxygen conditions. *Journal of Tissue Engineering*, 9, 204173141775371. <https://doi.org/10.1177/2041731417753718>
- Davisson, T., Sah, R. L., & Ratcliffe, A. (2002). Perfusion increases cell content and matrix synthesis in chondrocyte three-dimensional cultures. *Tissue Engineering*, 8(5), 807–816. <https://doi.org/10.1089/10763270260424169>
- Devarapalli, M., Lawrence, B. J., & Madhally, S. V. (2009). Modeling nutrient consumptions in large flow-through bioreactors for tissue engineering. *Biotechnology and Bioengineering*, 103(5), 1003–1015. <https://doi.org/10.1002/bit.22333>
- Elsaesser, A. F., Bermueller, C., Schwarz, S., Koerber, L., Breiter, R., & Rotter, N. (2014). In vitro cytotoxicity and in vivo effects of a decellularized xenogeneic collagen scaffold in nasal cartilage repair. *Tissue Engineering Part A*, 20(11–12), 1668–1678. <https://doi.org/10.1089/ten.TEA.2013.0365>
- Elsaesser, A. F., Schwarz, S., Joos, H., Koerber, L., Brenner, R. E., & Rotter, N. (2016). Characterization of a migrative subpopulation of adult human nasoseptal chondrocytes with progenitor cell features and their potential for in vivo cartilage regeneration strategies. *Cell & Bioscience*, 6, 11. <https://doi.org/10.1186/s13578-016-0078-6>
- Eyre, D. R., & Muir, H. (1975). The distribution of different molecular species of collagen in fibrous, elastic and hyaline cartilages of the pig. *Biochemical Journal*, 151(3), 595–602. <http://www.ncbi.nlm.nih.gov/pubmed/766752>
- Gaggioli, C., Hooper, S., Hidalgo-Carcedo, C., Grosse, R., Marshall, J. F., Harrington, K., & Sahai, E. (2007). Fibroblast-led collective invasion of carcinoma cells with differing roles for RhoGTPases in leading and following cells. *Nature Cell Biology*, 9(12), 1392–1400. <https://doi.org/10.1038/ncb1658>
- Goldberg-Bockhorn, E., Schwarz, S., Elsässer, A., Seitz, A., Körber, L., Dürselen, L., Ignatius, A., Feldmann, E.-M., Scheithauer, M., Breiter, R., & Rotter, N. (2014). Physical characterization of decellularized cartilage matrix for reconstructive rhinosurgery. *Laryngo-Rhino-Otologie*, 93(11), 756–763. <https://doi.org/10.1055/s-0034-1384531>
- Goldberg-Bockhorn, E., Schwarz, S., Subedi, R., Elsässer, A., Riepl, R., Walther, P., Körber, L., Breiter, R., Stock, K., & Rotter, N. (2018). Laser surface modification of decellularized extracellular cartilage matrix for cartilage tissue engineering. *Lasers in Medical Science*, 33(2), 375–384. <https://doi.org/10.1007/s10103-017-2402-8>
- Hamada, T., Sakai, T., Hiraiwa, H., Nakashima, M., Ono, Y., Mitsuyama, H., & Ishiguro, N. (2013). Surface markers and gene expression to characterize the differentiation of monolayer expanded human articular chondrocytes. *Nagoya Journal of Medical Science*, 75(1–2), 101–111. <http://www.ncbi.nlm.nih.gov/pubmed/23544273>
- Jiang, Y., Cai, Y., Zhang, W., Yin, Z., Hu, C., Tong, T., Lu, P., Zhang, S., Neculai, D., Tuan, R. S., & Ouyang, H. W. (2016). Human cartilage-derived progenitor cells from committed chondrocytes for efficient cartilage repair and regeneration. *Stem Cells Translational Medicine*, 5(6), 733–744. <https://doi.org/10.5966/sctm.2015-0192>
- Kellner, K., Liebsch, G., Klimant, I., Wolfbeis, O. S., Blunk, T., Schulz, M. B., & Göpferich, A. (2002). Determination of oxygen gradients in

- engineered tissue using a fluorescent sensor. *Biotechnology and Bioengineering*, 80(1), 73–83. <https://doi.org/10.1002/bit.10352>
- Khan, A. A., Suits, J. M. T., Kandel, R. A., & Waldman, S. D. (2009). The effect of continuous culture on the growth and structure of tissue-engineered cartilage. *Biotechnology Progress*, 25(2), 508–515. <https://doi.org/10.1002/btpr.108>
- Kim, H.-S., Park, S.-S., Kim, M.-H., Kim, M.-S., Kim, S.-K., & Lee, K.-C. (2014). Problems associated with alloplastic materials in rhinoplasty. *Yonsei Medical Journal*, 55(6), 1617–1623. <https://doi.org/10.3349/ymj.2014.55.6.1617>
- Koelling, S., Kruegel, J., Irmer, M., Path, J. R., Sadowski, B., Miro, X., & Miosge, N. (2009). Migratory chondrogenic progenitor cells from repair tissue during the later stages of human osteoarthritis. *Cell Stem Cell*, 4(4), 324–335. <https://doi.org/10.1016/j.stem.2009.01.015>
- Lepiarz, T., Wenzel, U., Hasch, K., Goldberg-Bockhorn, E., Rotter, N., & Hessling, M. (2017). Computational analysis of histological images of tissue engineered cartilage for evaluation of scaffold cell migration. *Journal of Biomedical Engineering and Medical Imaging*, 4(6), 01. <https://doi.org/10.14738/jbemi.46.3854>
- Liang, X., Wang, K., Malay, S., Chung, K. C., & Ma, J. (2018). A systematic review and meta-analysis of comparison between autologous costal cartilage and alloplastic materials in rhinoplasty. *Journal of Plastic, Reconstructive & Aesthetic Surgery*, 71(8), 1164–1173. <https://doi.org/10.1016/j.bjps.2018.03.017>
- Luo, L., Eswaramoorthy, R., Mulhall, K. J., & Kelly, D. J. (2015). Decellularization of porcine articular cartilage explants and their subsequent repopulation with human chondroprogenitor cells. *Journal of the Mechanical Behavior of Biomedical Materials*, 55, 21–31. <https://doi.org/10.1016/j.jmbbm.2015.10.002>
- Mabvuure, N., Hindocha, S., & Khan, W. S. (2012). The role of bioreactors in cartilage tissue engineering. *Current Stem Cell Research and Therapy*, 7(4), 287–292. <http://www.ncbi.nlm.nih.gov/pubmed/22563665>
- Magliaro, C., Mattei, G., Iacoangeli, F., Corti, A., Piemonte, V., & Ahluwalia, A. (2019). Oxygen consumption characteristics in 3D constructs depend on cell density. *Frontiers in Bioengineering and Biotechnology*, 7, 251. <https://doi.org/10.3389/fbioe.2019.00251>
- Mischkowski, R. A., Domingos-Hadamitzky, C., Siessegger, M., Zinser, M. J., & Zoller, J. E. (2008). Donor-site morbidity of ear cartilage autografts. *Plastic and Reconstructive Surgery*, 121(1), 79–87.
- Pierre, J., Gemmiti, C. V., Kolambkar, Y. M., Oddou, C., & Guldborg, R. E. (2008). Theoretical analysis of engineered cartilage oxygenation: Influence of construct thickness and media flow rate. *Biomechanics and Modeling in Mechanobiology*, 7(6), 497–510. <https://doi.org/10.1007/s10237-007-0107-9>
- Popko, M., Bleys, R. L. A. W., De Groot, J.-W., & Huizing, E. H. (2007). Histological structure of the nasal cartilages and their perichondrial envelope. I. The septal and lobular cartilage. *Rhinology*, 45(2), 148–152. <http://www.ncbi.nlm.nih.gov/pubmed/17708463>
- Princz, S., Wenzel, U., Schwarz, S., Rotter, N., & Hessling, M. (2016). New bioreactor vessel for tissue engineering of human nasal septal chondrocytes. *Current Directions in Biomedical Engineering*, 2(1), 319–322. <https://doi.org/10.1515/cdbme-2016-0071>
- Princz, S., Wenzel, U., Tritschler, H., Schwarz, S., Dettmann, C., Rotter, N., & Hessling, M. (2017). Automated bioreactor system for cartilage tissue engineering of human primary nasal septal chondrocytes. *Biomedical Engineering*, 62(5), 481–486. <https://doi.org/10.1515/bmt-2015-0248>
- Rowland, C. R., Colucci, L. A., & Guilak, F. (2016). Fabrication of anatomically-shaped cartilage constructs using decellularized cartilage-derived matrix scaffolds. *Biomaterials*, 91, 57–72. <https://doi.org/10.1016/j.biomaterials.2016.03.012>
- Schwarz, S., Elsaesser, A. F., Koerber, L., Goldberg-Bockhorn, E., Seitz, A. M., Bermueller, C., Dürselen, L., Ignatius, A., Breiter, R., & Rotter, N. (2015). Processed xenogenic cartilage as innovative biomatrix for cartilage tissue engineering: Effects on chondrocyte differentiation and function. *Journal of Tissue Engineering and Regenerative Medicine*, 9(12). <https://doi.org/10.1002/term.1650>
- Schwarz, S., Koerber, L., Elsaesser, A. F., Goldberg-Bockhorn, E., Seitz, A. M., Dürselen, L., Ignatius, A., Walther, P., Breiter, R., & Rotter, N. (2012). Decellularized cartilage matrix as a novel biomatrix for cartilage tissue-engineering applications. *Tissue Engineering Part A*, 18(21–22), 2195–2209. <https://doi.org/10.1089/ten.tea.2011.0705>
- Shahin, K., & Doran, P. M. (2011). Strategies for enhancing the accumulation and retention of extracellular matrix in tissue-engineered cartilage cultured in bioreactors. *PLoS One*, 6(8), e23119. <https://doi.org/10.1371/journal.pone.0023119>
- Swinehart, I. T., & Badyak, S. F. (2016). Extracellular matrix bioscaffolds in tissue remodeling and morphogenesis. *Developmental Dynamics*, 245(3), 351–360. <https://doi.org/10.1002/dvdy.24379>
- Tonnarelli, B., Santoro, R., Adelaide Asnaghi, M., & Wendt, D. (2016). Streamlined bioreactor-based production of human cartilage tissues. *European Cells and Materials*, 31, 382–394. <https://doi.org/10.22203/eCM.v031a24>
- Varadharajan, K., Sethukumar, P., Anwar, M., & Patel, K. (2015). Complications associated with the use of autologous costal cartilage in rhinoplasty: A systematic review. *Aesthetic Surgery Journal*, 35(6), 644–652. <https://doi.org/10.1093/asj/sju117>
- Yamada, K. M., & Sixt, M. (2019). Mechanisms of 3D cell migration. *Nature Reviews Molecular Cell Biology*, 20, 738–752. <https://doi.org/10.1038/s41580-019-0172-9>
- Zhou, S., Cui, Z., & Urban, J. P. G. (2008). Nutrient gradients in engineered cartilage: Metabolic kinetics measurement and mass transfer modeling. *Biotechnology and Bioengineering*, 101(2), 408–421. <https://doi.org/10.1002/bit.21887>

How to cite this article: Goldberg-Bockhorn, E., Wenzel, U., Theodoraki, M.-N., Döschner, J., Riepl, R., Wigand, M. C., Brunner, C., Heßling, M., Hoffmann, T. K., Kern, J., & Rotter, N. (2022). Enhanced cellular migration and prolonged chondrogenic differentiation in decellularized cartilage scaffolds under dynamic culture conditions. *Journal of Tissue Engineering and Regenerative Medicine*, 16(1), 36–50. <https://doi.org/10.1002/term.3261>